INTERNATIONAL JOURNAL OF AUTOMOTIVE AND MECHANICAL ENGINEERING (IJAME)
ISSN: 2229-8649 e-ISSN: 2180-1606
VOL. 17, ISSUE 3, 8168 – 8178
DOI: https://doi.org/10.15282/ijame.17.3.2020.10.0614

ORIGINAL ARTICLE

The Influence of Non-Pneumatic Tyre Structure on its Operational Properties

Z. Hryciów, J. Jackowski and M. Żmuda*

Institute of Vehicle & Transportation, Faculty of Mechanical Engineering, Military University of Technology,
2 Sylwestra Kaliskiego Street, 00-908 Warsaw, Poland
Phone: +48 261 839 565; Fax: +48 261 837 366

ABSTRACT – A non-pneumatic tyre (NPT) is a novel type of safety tyre that is designed to provide similar elastic properties to those offered by conventional pneumatic tyres. The main advantage of NPT is the lack of compressed air (like in a pneumatic tire) to ensure adequate traction forces and directional control. Suitable materials and the appropriate geometry of the supporting structure allows to achieve properties provides by pneumatic tires. Flexible spokes and closed structure like honeycomb are the most common solutions of supporting structure. Appropriate geometry, thickness and materials of this part affect the NPT properties; radial stiffness, unit pressure in the contact patch and the parameters of an area in contact with a non-deformable surface. The paper presents the FEM NPT model (NPT_0), which was validated with the results of experimental research of NPT. The NPT_0 model is subject to further modifications (layout and shape of the radial spokes) was used in the study. Seven new geometries of NPT supporting structure were selected for simulation tests. During the numerical tests the radial stiffness, unit pressure in the contact patch and the parameters of an area in contact with a non-deformable surface were determined. It has been observed that an increase in the curvature of the spokes reduced radial stiffness and increased the length of the contact path.

ARTICLE HISTORY
Revised: 14th Sept 2020
Accepted: 21st Sept 2020

KEYWORDS
Non-pneumatic tyre;
Airless tyre;
Radial stiffness characteristics;
NPT footprint;
NPT pressure in the contact patch

INTRODUCTION

Over the last few years, the rapid development of new types of tyres has been observed. One of the designs is referred to as a non-pneumatic tyre (NPT), an airless tyre, an elastic wheel, a non-solid tyre or a cushion tyre. One of the main advantages of an NPT is to prevent a vehicle from being immobilised by damage or a puncture while providing handling properties that are similar to those offered by conventional pneumatic tyres. The elastic properties of a pneumatic tyre depend on the pressure in the tyre [1–3] - a factor (drawback) that does not occur in non-pneumatic tyres. The appropriate definition of an NPT can be found in the regulation [4]; the US federal government regulations define NPTs as mechanical devices which transfer forces (both tangential and normal) from a road to a vehicle, as well as providing directional control and generating traction forces. Achieving the aforementioned tasks does not require a compressed gas or fluid to be maintained in the tyre.

The advantages of non-pneumatic tyres include being maintenance-free, good impact resistance, the ability to operate with a partially damaged tyre, and use in extreme terrain (e.g. rocky deserts). The disadvantages of NPTs include a high purchase price; the pressure cannot be adjusted to suit a particular surface and, at present, there are no designs that can achieve high-speed travel. Adjusting the unit pressure in a tyre can be implemented by a central tyre inflation system (CTIS) [5]. The use of this system for pneumatic tyres allows special vehicles (e.g. military vehicles) to move in low-grip terrain. Its use in commercial vehicles (e.g. a van) is able to reduce fuel consumption by adapting the inflation pressure to the vehicle's load [5]. Shaping the pressure and energy losses in the case of an NPT is limited to the selection of the appropriate geometry of the support structure and materials. Based on an analysis of the information in NPT brochures that are commercially available, the maximum speed for an NPT used in construction machinery is up to 15 km/h, while for utility terrain vehicles (UTV) it is up to 80 km/h [6]. On the basis of the literature review, it can be stated that all designs of NPTs include the following components (Figure 1) [7–13]: a tread, a shear beam (analogue to the carcass in a pneumatic tyre) or an elastic ring, a deformable supporting structure and a rim. The tyre's rim and tread perform the same functions as those in conventional pneumatic tyres. The shear beam may include a core (solid or of a specified geometry) between, e.g. two membranes (usually made from metal) that possess a low deformation modulus.

The air pressure in a conventional pneumatic tyre is represented in an NPT by the use of suitable materials and the appropriate design of the supporting structure (the shear beam) [11]. The most common shear beam that is used in numerical simulations consists of a core and suitable reinforcement. The core can be made from a solid elastomer (this provides passenger comfort during driving as well as high energy losses due to its high internal damping) or from a reduced volume of a specified material (with a specified geometry) [14]. Phromjan and Suvanjumrat [15] investigated the cross-section shear band of a commercial NPT. The shear beam was made from a combination of an elastomer and layers of cord thread; suitable results were obtained by using shell elements to simulate the cord threads. Ju et al. [14] conducted numerical tests on five NPTs with different cell configurations of a honeycomb shear beam made from

*CORRESPONDING AUTHOR | M. Żmuda | ✉ marcin.zmuda@wat.edu.pl

polycarbonate and mild-steel. The structures and materials that were used were intended to replicate the flexible shear properties of an elastomer. It has been shown that an auxetic honeycomb is a structure that can be used as a shear beam in the construction of NPTs. Ju et al. [16] presented the results of NPT simulation tests (length of the contact patch and unit pressure). The NPTs that were tested were equipped with a solid core and a specific geometry (a honeycomb with a different negative cell angle and length of the cell's side). The core allowed a longer contact patch to be obtained as well as small values of unit pressure (almost regular) for the NPT. The specific geometry of the core shortened the contact patch and increased the unit pressure with several peak values. The value of the unit pressure of an NPT with a solid core is directly proportional to the shear modulus G of the core material and the height of the shear beam and is inversely proportional to the external radius of the shear beam [11].

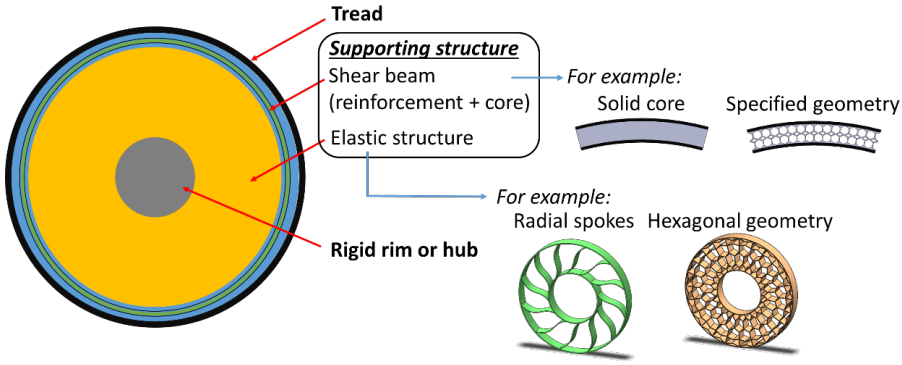

Figure 1. The general design of an NPT.

Jin et al. [17] carried out selected static and dynamic numerical simulation of an NPT with a hexagonal (honeycomb) support structure and a solid shear beam (steel reinforcement and a polyurethane core). The geometry of the honeycomb cells and the thickness of the spokes were modified by the authors. They observed that, for the same spoke thickness and a different geometry of the honeycomb cell, the displacement of the centre of the NPT under the applied normal force reached similar values. A significant difference occurred at high values of the normal force (approximately 4 kN). The displacement of the centre of the NPT was influenced by the value of its radial stiffness. Kim et al. [8] optimised the structure of an NPT to minimise its rolling resistance. Their numerical model of the NPT included a shear beam with a solid core and hexagonal spokes. The constraints adopted by the authors were the vertical displacement and the maximum contact pressure, while changes were made to i.a. the thickness of the shear beam and the spokes. They observed that the radial stiffness of the NPT increased when the thickness of the shear beam or the thickness of the spokes was increased. This was caused by the increase in the volume of the material and its resistance to deformation. In addition, the maximum contact pressure has been shown to be proportional to the thickness of the shear beam or the spokes.

Kucewicz et al. [18] conducted numerical tests of an NPT with different spokes (four variants: two with single spokes, one with honeycomb spokes, one with mixed geometry of the spokes – the authors' geometry). The shear beams for all of the tested NPTs were modelled as a single reinforcement layer as the cord layer – using beam elements (similar to a pneumatic tyre's cord layer). The results demonstrated the influence of the spokes' geometry on the value of the NPT's centre displacement (radial stiffness); the NPT equipped with spokes with a greater curvature showed greater susceptibility to vertical displacement of the wheel's centre. Vinay et al. [19] carried out numerical tests on an NPT with hexagonal spokes and noted that changes in the honeycomb's geometry affected the vertical displacement values. The reduction in the spokes deformation due to the normal force was a result of the increase in the spokes' thickness. A comparison of the masses of the individual NPT's elements revealed that approximately 80 % of the total mass consisted of the mass of the tread and the supporting structure (the shear beam and the spokes). The aforementioned parts of the NPT are cyclically loaded and deform during movement of a vehicle; a large volume of material cause large energy losses. Therefore, reducing the mass of the wheel, while maintaining its high fatigue resistance, is desirable.

Rugsaj and Suvanjumrat [12] developed a numerical model of a commercially available NPT with single spokes. The material data for the model was obtained as a result of laboratory tests that were carried out on specimens of the NPT. The numerical simulations were aimed at selecting the optimal thickness of a single spoke to mimic the radial characteristics of a pneumatic tyre. A nearly linear increase in the NPT's radial stiffness was observed as a result of increasing the spoke thickness. Zhao et al. [20] presented numerical and experimental studies on their own ideas (a mechanical elastic wheel); their research investigated the wheel's radial stiffness and natural frequency as an effect of the driving torque. The interesting solution that they found, which is different from those encountered in other studies, is their representation of the spokes as a group of hinges. This solution eliminated the energy loss that is associated with the cyclical deformation of this part of the NPT. The shear beam was presented as a group of elastic outer rings combined in one layer. It has been observed that the properties of the materials that are used affect selected characteristics of the wheel, e.g. by increasing the elastic modulus of the elastic rings, the natural frequency of the wheel increased.

Zhou et al. [21] pointed out the problem of noise generated by an NPT with single spokes. The use of a non-smooth surface (riblet) on the spokes or the NPT's external ring can reduce aerodynamic noise. Noise reduction is important due to its negative effect on the environment and people. The load-carrying capacity of an NPT is several times higher than that of a solid tyre of the same size, due to its different mode of normal load transfer. A solid tyre transfers the load

directly at the contact patch [11]; this load transfer mode is referred to as a 'bottom loader'. Loading the NPT with a normal force results in elastic buckling of the structural elastic elements below the tyre's axis and stress/tension in the area above the tyre's axis. This mode of load transfer is referred to as a top loader, see Figure 2.

In this mode, the shear beam is deformed around its entire perimeter [10, 20, 22]. The state of this deformation depends on the stiffness of the elastic structure, the material properties and the tyre's geometry, see Figure 3. The aforementioned load-carrying mechanics concern an NPT equipped with single (flat or curved) spokes. An NPT with spokes of specified geometry– forming closed cells - (e.g. hexagonal spokes, rhombi tessellated spokes) indicates a bottom loading phenomenon. This load-carrying mechanics characteristic was presented by Kumar and Krishna Kuma [23] as a stress distribution of the rhombi tessellated spokes during a simulation of the radial stiffness of an NPT.

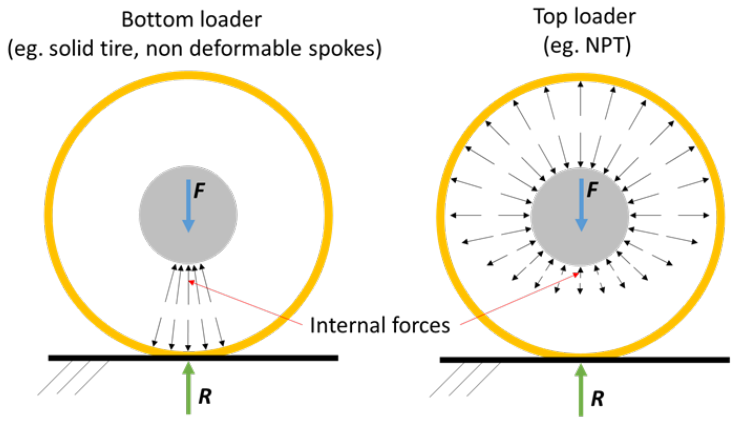

Figure 2. Comparison of the mechanics of bottom and top loader load-carrying.

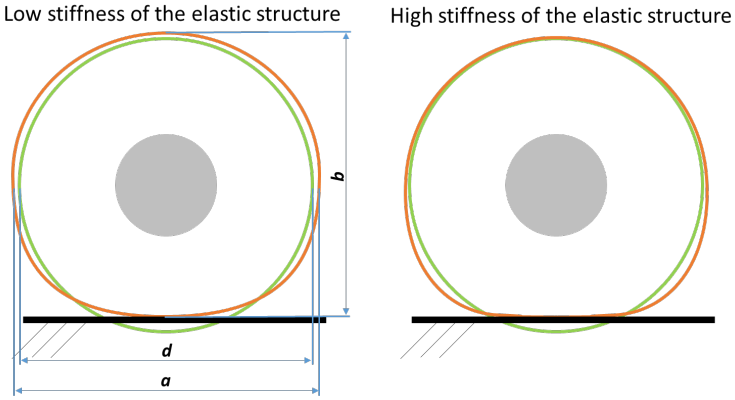

Figure 3. Effects of the flexible elasticity of the shear beam on the deformation of the outer layer of the tyre (nominal tyre diameter shown in green).

Numerical simulations require the use of the appropriate material constitutive models. Most of an NPT is constructed from an elastomer, which is characterised by large non-linearity. When choosing a suitable constructive model, the strain value should be identified. For small strains (i.e. up to 10%), the best mapping is given by the Neo-Hookean model; in the range of strain from 10% to 300%, the Mooney-Rivlin model is recommended. The Yeoh model is usually chosen for large strain values in elastomers (up to 700%) [24], [25].

The novelty in this paper is the assessment of the influence of the different shapes of the spokes in commercially available NPTs on selected properties of the NPTs (e.g. radial characteristics, footprint and length of the contact patch). This research was aimed at assessing the influence of different single spokes in the 3D finite element NPT model on selected operational properties. Simulation tests were carried out to identify the phenomena that occur during the loading of an NPT and to evaluate the effects of the elastic geometry (a deformable supporting structure) on the radial characteristics, the shear beam's deformation and the parameters of the contact patch (contact patch length and unit pressure).

NUMERICAL NPT MODELS

Figure 4 shows a non-pneumatic tyre and its model (initial variant NPT_0). The LS-DYNA software was used for the numerical simulations; it is finite element method software which is widely used to analyse physical phenomena, in particular mechanics. Among other applications, LS-DYNA can be used to solve highly non-linear statics and dynamics problems. The whole NPT model consisted of more than 32,000 shell and 25,000 solid elements.

Figure 4. The non-pneumatic (a) tyre and its (b) model (NPT_0).

The model (NPT_0) consisted of the tread, the shear beam and 50 radial spokes arranged between two rings as shown in Figure 5. The fully integrated shell element approximation method was used to model the spokes. The thickness of the spokes was assumed to be constant (7 mm) over their total length. The shear beam consisted of two materials: solid core elements (elastomer) and two layers of reinforcement (steel). The solid core was modelled using 8-node hexahedron elements, whereas the reinforcement was modelled using membrane elements. Therefore only the translational degrees-of-freedom (reinforcement elongation) contributed to the strain in the membrane. The reinforcement layers were modelled using a linear elastic material with a modulus of elasticity (E) of 200 GPa and a Poisson's ratio of 0.3. A 'hyper-viscoelastic rubber' material model was used to define the hyperelastic properties of the spokes, the shear beam's core and the tread. Depending on the number of coefficients that were used, the model behaved as either a Mooney-Rivlin model or a Neo-Hookean model [26].

$$W(J_1, J_2) = \Sigma\, C_{pq}(J_1 - 3)^p (J_2 - 3)^q + W_H(J) \quad (1)$$

Where, W – the strain energy density function, C_{pq} – the material constant (p and q - take the values: 0 or 1 which results in C_{01}, C_{10}), J_1, J_2 – the Cauchy-Green deformation tensor invariant, W_H (J) - hydrostatic work (an expression of the strain-energy function).The material data used in the numerical model (Table 1) was taken from the literature [27–29]. The shear beam reinforcement was represented by the anisotropic material model.

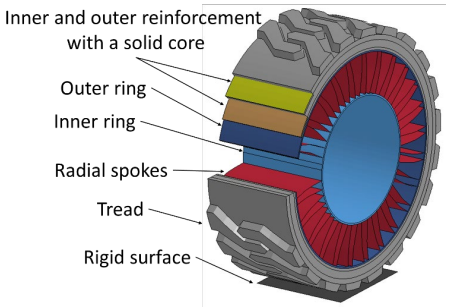

Figure 5. Diagram of the NPT_0 numerical model.

During the vertical stiffness testing, the FE model of the NPT acted on a rigid surface (the tyre testing machine's plate in the experiment). Coulomb's friction model was used to calculate the friction force that occurred between the tread elements and the rigid surface with a friction coefficient of 0.8. The rigid surface was assigned as fixed and a force pressing the NPT against the surface was applied; the developed model was then verified in the experimental tests. Figure 6 shows the test bench used for the tested NPT; a detailed description of the test bench can be found in the literature [30, 31]. During the experimental tests, a load was applied to the wheel on a rigid surface. Loading was carried out by changing the distance between the NPT's axis of rotation and the rigid surface; the normal force was measured using a force transducer. The test bench could produce loads of normal force up to 60000 N and longitudinal and lateral forces of up to 50000 N [31]. The accuracy of the measured load was 0.01 N, and the NPT's displacement was measured using linear variable differential transformer (LVDT) displacement sensors with an accuracy of 0.01 mm. Figure 7 shows the model's validation results; the results of the numerical test and the experimental test were well matched. Model validation is described in [32].

Table 1. Material coefficients for the material model [27–29].

Model element	Material model	Poisson's ratio	C_{10} (MPa)	C_{01} (MPa)
Radial spokes	Mooney-Rivlin	0.4500	10.0586	7.7445
Shear beam	Neo-Hookean	0.4821	0.8330	-
Tread	Neo-Hookean	0.4821	0.5000	-

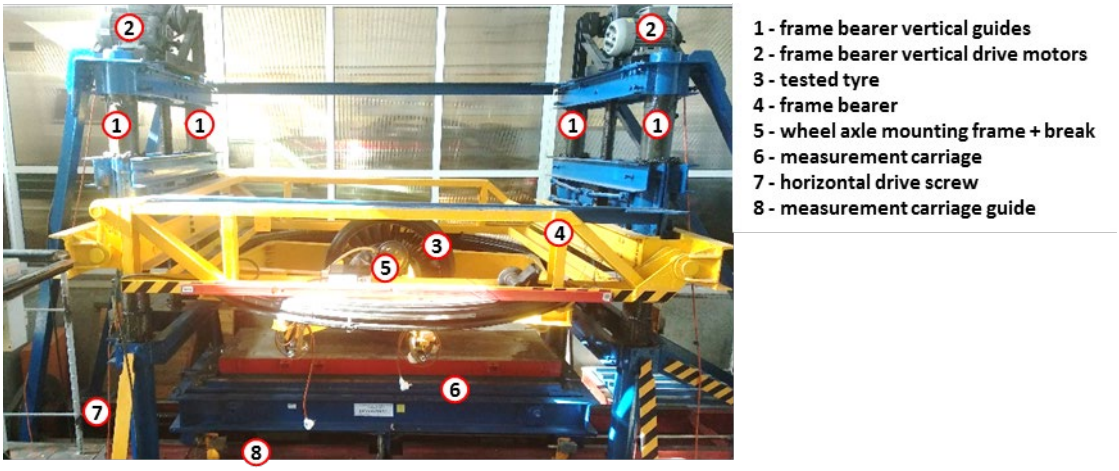

Figure 6. A universal quasi-static indoor tyre test bench with NPT.

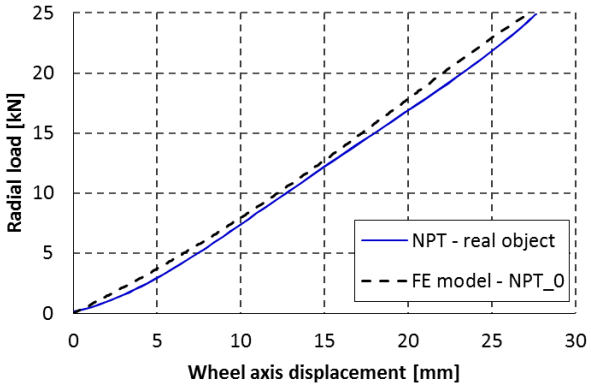

Figure 7. Test results of the NPT_0 model and the experimental tests - radial characteristics.

At the next stage, the NPT_0 model was modified in the area of the deformable supporting structure. The shape of the spokes and the points where they were attached to the inner and outer membrane were modified. The number of spokes and the other elements of the tyre's model were not modified (they were the same as in model NPT_0); Figure 8 shows the NPT_1 - NPT_7 versions. The attachment points of the spokes to the outer (9) and inner (8) rings in all of the new models were evenly distributed around the circumference of the wheel.

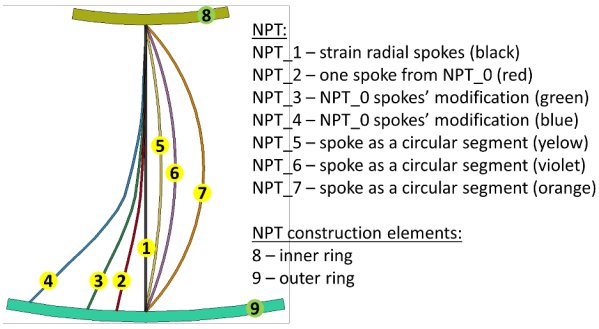

Figure 8. Geometry of the spokes in the numerical models of the NPT.

NUMERICAL TEST RESULTS

The numerical tests were carried out with a 20 kN normal load, corresponding to the tyre's load in a vehicle fitted with non-pneumatic tyres. The scope of the tests included the following measurements: the radial stiffness characteristics, the unit pressure in the contact patch on a non-deformable surface, the length of the contact patch and the deformation of the tyre's outer layer.

In order to determine the radial characteristics, the NPT was loaded to 125% of the nominal load and then the load was removed. For the recorded hysteresis loop, a centre line was constructed which was then used to calculate the stiffness in the characteristic point corresponding to 100% of the nominal load. The contact patch parameters and unit pressures

were determined for a load equal to 100% of the normal load. The average value of unit pressure in the contact patch was determined as the quotient of the sum of unit pressure elements exerted on finite elements of rigid surface to the sum of the surfaces of these elements.

Figure 9 and Table 2 show the results of the radial stiffness characteristics for the different designs of the supporting structure. The test results show a decrease in the radial stiffness when the curvature (and length) of the spokes was increased. Within the scope of the modifications, for the models featuring spokes with the highest curvature (NPT_4 and NPT_7 models), the radial stiffness was reduced by almost twofold (compared to NPT_0). For NPT_1 the stiffness characteristic was non-linear; for loads up to approximately 7 000 N, the stiffness was approximately 10% higher compared to that observed at higher loads due to sudden elastic buckling of the spokes below the tyre's axis. Before the elastic buckling occurred, the load was transferred from the compressed spokes below the tyre's axis to the spokes under tension above the tyre's axis.

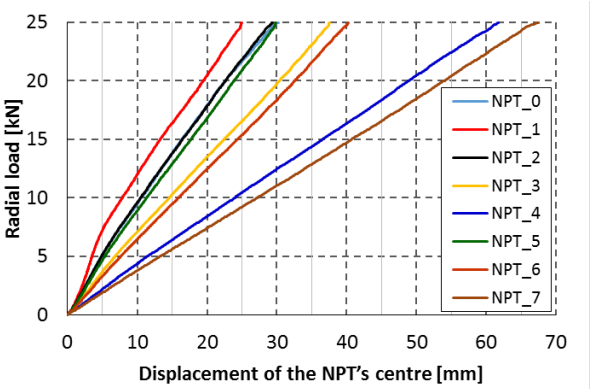

Figure 9. Radial stiffness characteristics (central line) for the NPT models.

Table 2. Numerical test results for the NPT models.

	NPT_0	NPT_1	NPT_2	NPT_3	NPT_4	NPT_5	NPT_6	NPT_7
Coefficient of radial stiffness (kN/m)	745.3	825.2	781.5	650.9	397.4	800.6	626.9	386.4
Average unit pressure in contact patch (kPa).	0.722	0.771	0.747	0.683	0.635	0.715	0.668	0.603
Contact patch length (mm)	216	213	209	223	260	209	232	255

It was observed that an increase in the spokes' curvature resulted in an increase in the deformation of the shear beam. As a result, the length of the contact patch increased, and the mean unit pressure at the contact patch decreased, see Table 2. Figure 10 shows the contact patch for the changes in the tread's load for all of the NPT models. Figure 11 shows the percentage change in the values of the evaluated parameters compared to the NPT_0 model. The changes in the evaluated parameters for all of the NPT models are closely related to a different mode of elastic buckling of the spokes that were adjacent to the contact patch and the tension of spokes on the opposite side of the wheel, see Figure 12. The deformation of the shear band at the contact patch changed the shape of the outer layer of the tyre, as shown in Table 3. The table shows the deformation of the outer layer that was measured as the difference between the distance between two points in the horizontal plane (distance a – see Figure 3) and two points in the vertical plane (distance b). The dimensions of a pneumatic tyre barely change under load, a (a=d), whereas the NPT showed significant deformation. Under the load, the NPT became oval, and in extreme cases (NPT_7) the dimension c (c=d-a) changed by 47 mm.

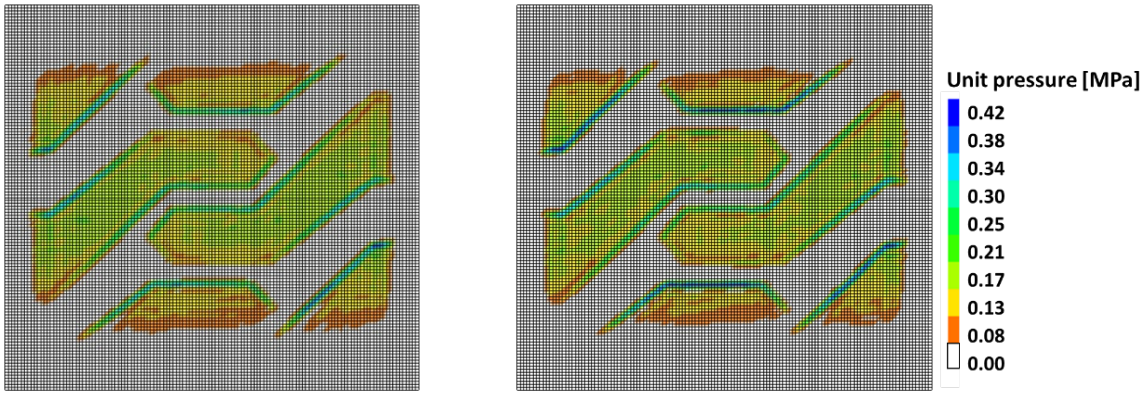

(a) NPT_0 (b) NPT_1

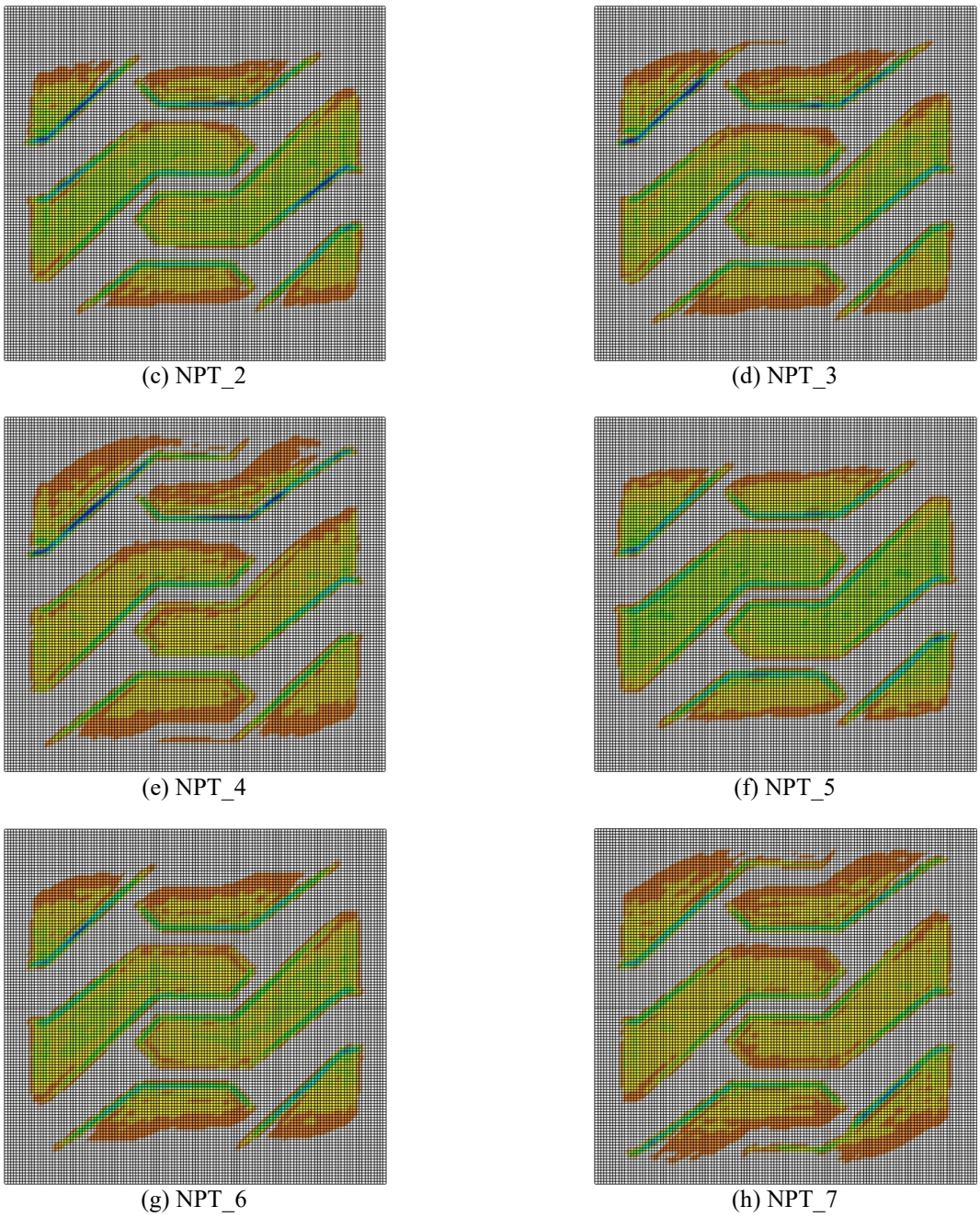

(c) NPT_2 (d) NPT_3

(e) NPT_4 (f) NPT_5

(g) NPT_6 (h) NPT_7

Figure 10. Unit pressure distribution in the contact patch of the NPT models on a non-deformable surface.

Figure 12 shows the details of the deformed (buckled) spokes that were directly below the tyre's axis. The smallest change between the outer and inner rings observed for NPT_1 (15 mm). NPT_0 and NPT_2 showed similar deformation of the spokes below the tyre's axis (18 mm). The spokes in the other models were more susceptible to deformation; under load, the deflection of the tyre, measured as the change in the distance from the tyre's axis to the surface, was as follows: NPT_3 – 25 mm, NPT_4 –42 mm, NPT_5 – 20 mm, NPT_6 – 30 mm and NPT_7 – 50 mm. The upper spokes were extended by: NPT_1 – 0.9 mm; NPT_2 – 1.4 mm; NPT_3 – 2.6 mm, NPT_4 – 6.0 mm, NPT_5 – 1.5 mm, NPT_6 – 2.8 mm and NPT_7 – 7.2 mm.

Table 3. Deformation of the tyre's outer layer (tread) in the vertical and horizontal axis under a normal force of 20 kN.

	NPT_0	NPT_1	NPT_2	NPT_3	NPT_4	NPT_5	NPT_6	NPT_7
Non-loaded tyre diameter d (mm)	840							
Distance a (mm)	842	842	842	844	850	843	845	852
Distance b (mm)	819	821	819	812	796	818	810	793
Deformation (mm)	21	19	21	28	44	22	30	47

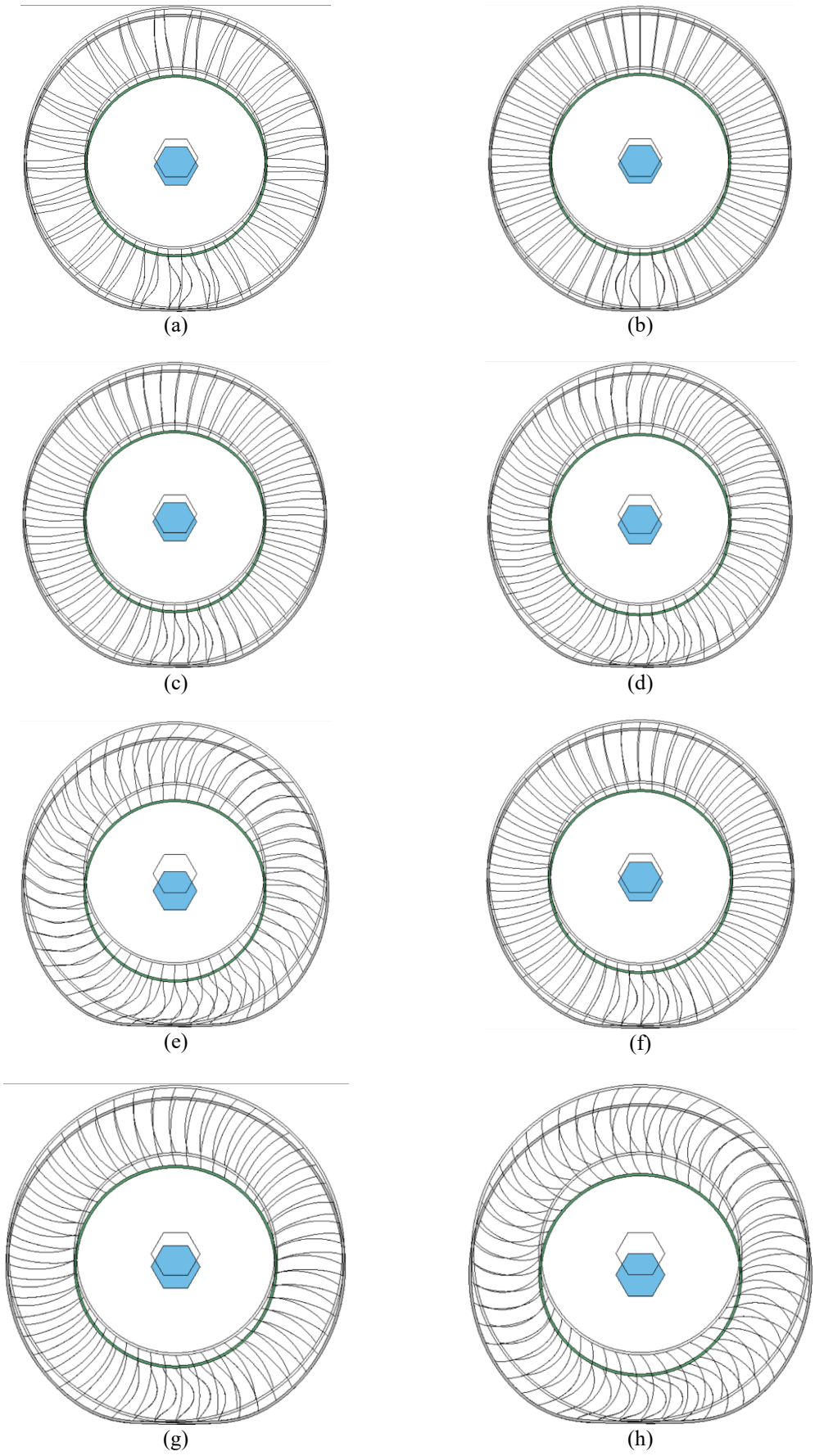

Figure 11. Spoke deformation under a 20 kN normal force: (a) NPT_0, (b) NPT_1, (c) NPT_2, (d) NPT_3, (e) NPT_4, (f) NPT_5, (g) NPT_6, (h) NPT_7.

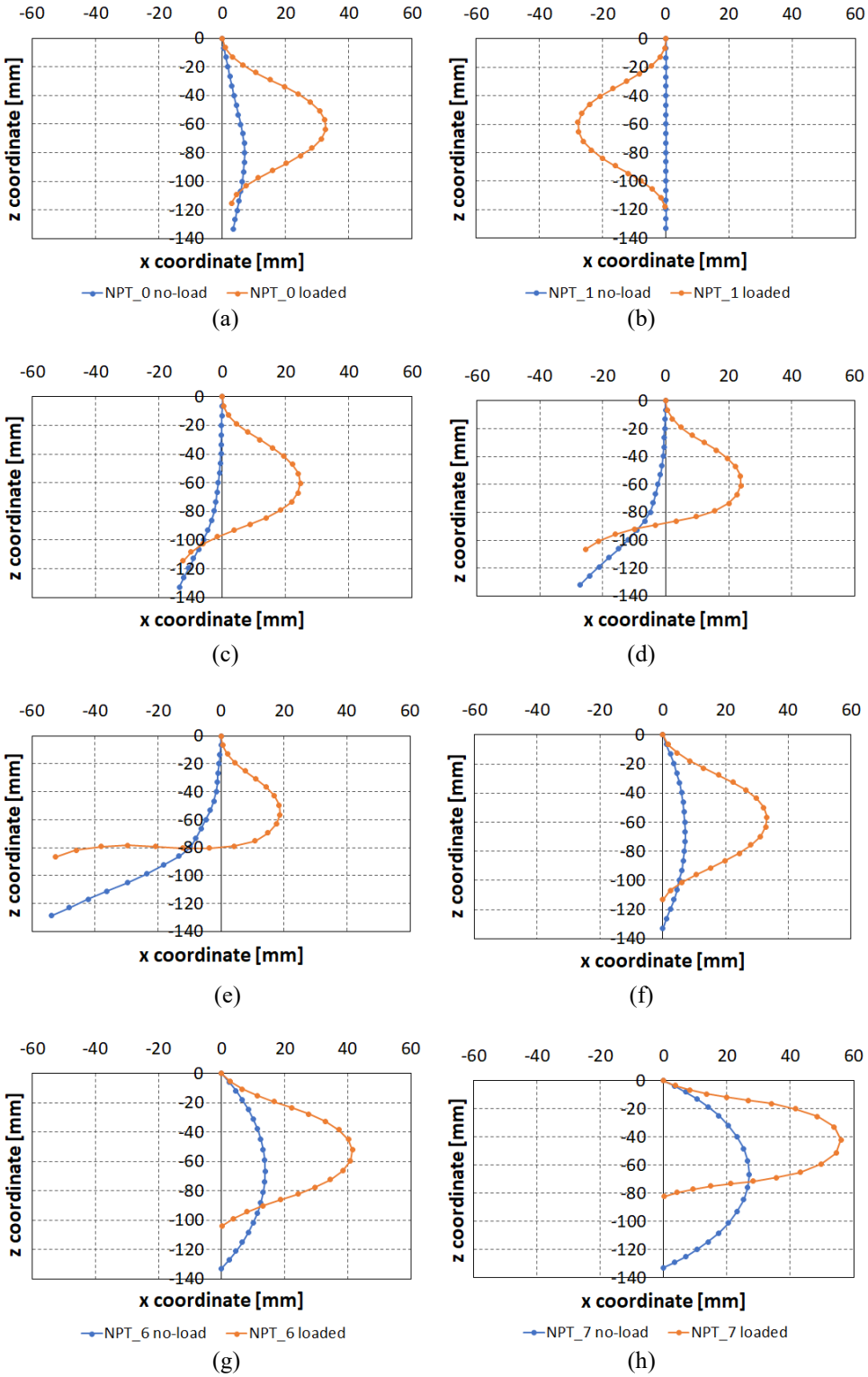

Figure 12. Radial elastic displacement of the spokes of the NPT models: (a) NPT_0, (b) NPT_1, (c) NPT_2, (d) NPT_3, (e) NPT_4, (f) NPT_5, (g) NPT_6 and (h) NPT_7.

CONCLUSION

In this paper, the influence of the structure of a non-pneumatic tyre on its operational properties has been investigated. The test results have allowed the effects of the shape of the spokes on the static properties of the NPT to be evaluated. It was found that an increase in the curvature (and length) of the spokes significantly decreased the radial stiffness of the tyre as a result of free (within the constraints of the curvature) elongation of the spokes above the tyre's axis of rotation. The length of the contact patch was extended when the stiffness of the supporting structure was lower. It can be expected that the deformation of a relatively large area of the supporting structure may contribute to increased internal friction, as well as a larger deformation hysteresis loop and, as a result, an increase in the rolling resistance; this was validated by the test results presented in the literature [33]. A design with the spokes arranged radially resulted in the simultaneous transfer

of the loads from the spokes in the upper section (tension) to the lower section (compression) until elastic buckling of the spokes in the lower section occurred. This resulted from the digressive characteristics of the tyre's radial stiffness. The radial characteristics provided information about the loads acting on the vehicle's body. Different values for the normal force were obtained from the same deflection of each NPT. When striving to reduce the load of the sprung mass of the vehicle, the best solution is an NPT; these produce large values of the displacement of the wheel's centre. Unfortunately, this is associated with large deformations of the wheel's geometry, which can translate into energy losses. The tests on the different designs of the NPTs allowed the following conclusions to be drawn.

i. Modifying the spokes' curvature may affect the elastic buckling of the spokes in the lower section of the tyre, as well as the tension in the upper section of the tyre and significantly affect the tyre's stiffness; the test results showed more than a twofold increase/decrease in the stiffness of the wheel, depending on the model,
ii. a low spoke curvature reduced the deformation of the shear beam, and
iii. the spoke curvature and length affected the parameters of the contact patch.

The test results in this paper are considered to be preliminary tests that will be used in the design and production of a non-pneumatic tyre with the required performance characteristics.

REFERENCES

[1] Besselink IJM, Schmeitz AJC, Pacejka HB. An improved Magic Formula/Swift tyre model that can handle inflation pressure changes. Vehicle System Dynamics 2010; 48: 337–52.

[2] Kulikowski K, Szpica D. Determination of directional stiffnesses of vehicles' tires under a static load operation. Eksploatacja i Niezawodność – Maintenance and Reliability 2014; 16(1): 66 - 72.

[3] Parczewski K. Effect of tyre inflation preassure on the vehicle dynamics during braking manouver. Eksploatacja i Niezawodnosc – Maintenance and Reliability 2013; 15(2): 134 – 139.

[4] 49 CFR § 571.129. Code of Federal Standard No. 129; New non-pneumatic tires for passenger cars. National Highway Traffic Safety Administration, Department of Transportation. Retrieved from: https://www.govinfo.gov/app/details/CFR-2011-title49-vol6/CFR-2011-title49-vol6-sec571-129; 07 April, 2020.

[5] D'Ambrosio S, Vitolo R, Salamone N, Oliva E. Active tire pressure control (ATPC) for passenger cars: design, performance, and analysis of the potential fuel economy improvement. SAE International Journal of Passenger Cars—Mechanical Systems 2018; 11: 1–18.

[6] Michelin ® X ® Tweel ® Airless Radial Tire Family. Retrieved from: https://www.michelintweel.com; 07 April, 2020.

[7] Du X, Zhao Y, Wang Q, Fu H, Lin F. Grounding characteristics of a non-pneumatic mechanical elastic tire in a rolling state with a camber angle. Strojniski Vestnik/Journal of Mechanical Engineering 2019; 5: 287-29

[8] Ju J, Veeramurthy M, Summers JD, Thompson L. Rolling resistance of a non-pneumatic tire having a porous elastomer composite shear band. Tire Science and Technology 2013; 41(3): 154-173.

[9] Kim K, Heo H, Uddin MS, Ju J, Kim DM. Optimisation of non-pneumatic tire with hexagonal lattice spokes for reducing rolling resistance. SAE Technical Papers: 2015-01-1515; 2015.

[10] Kim K, Kim DM, Ju J. Static contact behaviors of a non-pneumatic tire with hexagonal lattice spokes. SAE International Journal of Passenger Cars—Mechanical Systems 2013; 6(3): 1518 – 1527.

[11] Rhyne TB, Cron SM. Development of a non-pneumatic wheel. Tire Science and Technology 2006; 34(3): 150-169.

[12] Rugsaj R, Suvanjumrat C. Proper radial spokes of non-pneumatic tire for vertical load supporting by finite element analysis. International Journal of Automotive Technology 2019; 20(4): 801-812.

[13] Xiao Z, Zhao YQ, Lin F, Zhu MM, Deng YJ. Studying the fatigue life of a non-pneumatic wheel by using finite-life design for life prediction. Strojniški vestnik - Journal of Mechanical Engineering 2018; 64(1): 56-67.

[14] Ju J, Summers JD, Ziegert J, Fadel G. Design of honeycomb meta-materials for high shear flexure. In: Proceedings of the ASME 2009 International Design Engineering Technical Conferences & Computers and Information in Engineering Conference IDETC/CIE 2009, San Diego, California, USA, pp. 1 – 10; 2009.

[15] Phromjan J, Suvanjumrat C. The modification of steel belt layer of airless tire for finite element analysis. IOP Conference Series: Materials Science and Engineering 2020; 773: 1 - 4.

[16] Ju J, Ananthasayanam B, Summers JD, Joseph P. Design of cellular shear bands of a non-pneumatic tire -investigation of contact pressure. SAE International Journal of Passenger Cars - Mechanical Systems 2010; 3: 598–606.

[17] Jin X, Hou C, Fan X, Sun Y, Lv J, Lu C. Investigation on the static and dynamic behaviors of non-pneumatic tires with honeycomb spokes. Composite Structures 2018; 187: 27–35.

[18] Kucewicz M, Baranowski P, Małachowski J. Airless tire conceptions modeling and simulations. In: Proceedings of the 13th International Scientific Conference 2017, Lecture Notes in Mechanical Engineering 2017: 293-301.

[19] Vinay TV, Marattukalam KJ, Varghese SZ, Samuel S, Sreekumar S. Modeling and analysis of non-pneumatic tyres with hexagonal honeycomb spokes. International Journal on Recent Technologies in Mechanical and Electrical Engineering (IJRMEE) 2015; 2(3): 19-24.

[20] Zhao Y qun, Zang L guo, Chen Y qiao, Li B, Wang J. Non-pneumatic mechanical elastic wheel natural dynamic characteristics and influencing factors. Journal of Central South University 2015;22:1707–15.

[21] Zhou H, Jiang Z, Yang J, Zhai H, Wang G. Numerical investigation of aerodynamic noise reduction of nonpneumatic tire using nonsmooth riblet surface. Applied Bionics and Biomechanics 2020; 1: 1-13.

[22] Deng Y, Zhao Y, Lin F, Xiao Z, Zhu M, Li H. Simulation of steady-state rolling non-pneumatic mechanical elastic wheel using finite element method. Simulation Modelling Practice and Theory 2018; 85: 60-79.

[23] Kumar AS, Kumar RK. Force and moment characteristics of a rhombi tessellated non-pneumatic tire. Tire Science and Technology 2016; 44(2): 130 – 148.

[24] Jaszak P. Modelowanie gumy za pomocą metody elementów skończonych. Elastomery 2016; 20 :31 – 39.

[25] Mann V, Dechwayukul C, Thongruang W, Srewaradachpisal S, Kaewpradit P, Apichai WK, et al. Design and fabrication of natural rubber lightweight spring for motorcycle's shock absorber. International Journal of Automotive and Mechanical Engineering 2020; 17(1): 7758–7770.
[26] Ls-Dyna® Keyword User's Manual 1 Volume Ii Material Models Ls-Dyna R8.0 03/18/15 (R:6307) Livermore Software Technology Corporation (LSTC), Issue Date: 21.01.2002.
[27] Baranowski P, Bogusz P, Gotowicki P, Małachowski J. Assessment of mechanical properties of offroad vehicle tire: Coupons testing and FE model development. Acta Mechanica et Automatica 2012; 6(2): 17-22.
[28] Veeramurthy M, Ju J, Thompson LL, Summers JD. Optimisation of a non-pneumatic tyre for reducing rolling resistance. International Journal of Vehicle Design 2014; 66(2): 193 - 216.
[29] Veeramurthy M. Modeling , finite element analysis , and optimisation of Non-Pneumatic Tire (NPT) for the minimisation of rolling resistance 2011. A Thesis Presented to The Graduate School of Clemson University, Clemson University 8-2011, 14. Retrieved from: https://tigerprints.clemson.edu/cgi/viewcontent.cgi?article=2154&context=all_theses; 07 April, 2020.
[30] Jackowski J, Wieczorek M. Analysis of interaction between tyre tread and road on the basis of laboratory test. In: 7th International Science Conference Transbaltica 2011, Vilnius, pp. 292 – 296; 2011.
[31] Luty W, Prochowski L, Szurkowski Z. Stanowisko do badań ogumienia dużego rozmiaru. In: VII Międzynarodowe Symp. IPM. Warszawa-Rynia, pp. 375 – 382; 1999.
[32] Żmuda M, Jackowski J, Hryciów Z. Numerical research of selected features of the non-pneumatic tire. AIP Conference Proceedings 2019; 2078: 020027-1 - 020027-8.
[33] Jackowski J, Wieczorek M, Żmuda M, Energy consumption estimation of non-pneumatic tire and pneumatic tire during rolling. Journal of KONES Powertrain and Transport 2018; 1(1): 159 – 168.